



ANALYTICAL ASSESSMENT OF THE VULNERABILITY OF UNDERGROUND JOINTED PVC PIPELINES TO FAULT DISPLACEMENTS

Radan IVANOV¹, Shiro TAKADA² and Norikazu MORITA³

SUMMARY

Field surveys of PVC pipelines exposed to earthquakes have repeatedly confirmed that very often damage occurs due to joint failure. The damage can be particularly severe when pipes cross faults.

A comprehensive numerical method for assessing the total damage of buried pipelines was developed. The pipe body is modelled by line elements, and plastic deformation within it considered by plastic hinges. Experimental joint behaviour data is used without any simplifying assumptions in order to make the overall pipeline response as realistic as possible. Soil-pipe interaction is modelled by elasto-plastic normal and drag soil springs. The performance of the program is verified against test data.

The influence of the main parameters affecting pipeline behaviour, namely pipe diameter, stiffness of surrounding soil, fault crossing location and fault crossing angle have been studied, vulnerability charts for common pipe diameters produced, and patterns of failure identified. Simplified equations for predicting the fault slip at failure are derived.

It was found that for fault crossing angles in the ranges 30° to 75° and 120° to 150° the failure modes are exclusively joint pull-out and joint compression. For these ranges the influence of soil stiffness and fault crossing location is negligibly small. The failure appears to depend simply on the amount of pull-out or compression allowance of the particular joint. On the other hand, for the range 75° to 120° the failure mode can vary from joint pull-out (up to 90°), through bending failure of the pipe body or joint (90° to 120°) to joint compression failure (120°), and the failure slip in this range can be between two and ten times as large as the failure slip at crossing angles 30° or 150°.

INTRODUCTION

The performance of utility pipelines is of major importance in determining the earthquake vulnerability of urban areas. Therefore, reliable estimates of the resistance of pipelines to earthquake effects are needed.

¹ Research Associate, Kobe University, Kobe, Japan. Email: radan@kobe-u.ac.jp

² Professor, Kobe University, Kobe, Japan. Email: takada@kobe-u.ac.jp

³ Graduate Student, Kobe University, Kobe, Japan. Email: 022t135n@y02.kobe-u.ac.jp

Field surveys of damages pipelines have repeatedly confirmed that a large proportion of the failures of jointed pipes occur at the joints. During the Kobe earthquake pipes in the vicinity of active faults sustained major damage [1], [2]. During the 1964 Niigata earthquake 68% of the water pipelines in the city sustained damage with joint detachment being the most prominent failure mode [3], [4]. There are many active faults in the Japan including such in urban areas, so the study of their performance during earthquake is important to disaster mitigation.

Currently the most commonly used pipes in Japan are the ductile cast iron and PVC pipes. The latter are favoured for their corrosion durability, ease of installation and hygiene. However, their seismic performance has not been studied in detail yet. In order to reliably evaluate the overall pipeline behaviour, we developed a comprehensive numerical method for failure simulation of buried pipelines and used it to produce fragility curves for the most commonly used diameters of PVC pipes. Further, we derived simplified equations for the prediction of the fault slip causing pipe failure based on the analysis results.

ANALYSIS METHOD

Closed form solutions to the pipe–soil interaction problem based on beam on elastic foundation theory have been proposed by Kennedy [5], and Wang [6]. Such methods are excellent for grasping the nature of the problem but cannot be applied when large deflections or material nonlinearities are present. The Finite Element Method (FEM) has been routinely applied for pipe analysis; numerous examples of beam, shell or combined models can be found in the literature, e.g. [7]. Transfer matrix methods have also been developed [8]. While the FEM analyses are successful in revealing most of the features of pipeline behaviour, rupture and detachment at joints cannot be dealt with; for the shell version the computation effort is too great to allow large models consisting of many pipe segments to be analysed. The main purpose of the proposed method is to extend the domain of pipeline analysis through the failure and post-failure stages, while taking advantage of the efficacy of simple line elements in the modelling.

Features of the method

Modelling of the pipe body

The model consists of lumped masses (elements) connected by sets of springs as shown in Fig. 1. Each spring set consists of an axial, bending and torsional components derived from beam theory. The general constitutive behaviour for axial forces implemented in the program is elasto-plastic with strain hardening. The constitutive behaviour in bending (plastic hinge formation) can be specified either as a piecewise linear, or a second order curve. When the bending behaviour is bilinear elasto-plastic, the influence of the axial force on plastic hinge formation is considered.

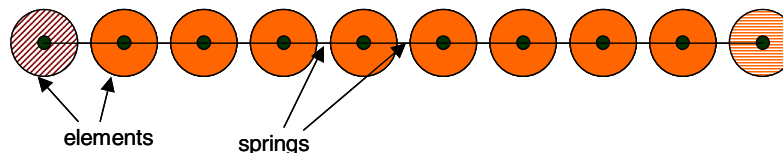


Fig. 1 Model of a pipe

Modelling of soil-pipe interaction

The soil surrounding the pipeline is modelled by pairs of springs having axial stiffness only, with one end attached to the pipe body and the other end fixed. The first spring is perpendicular to the pipe and represents the direct contact between pipe and soil; the other is tangential to the pipe and represents the drag between pipe and soil. Input displacements are specified at the fixed ends to simulate fault displacements. The direct soil springs are active only in compression, whereas the drag springs are active in both directions of relative displacement between pipe and soil. The direction of all soil springs is modified at each time step to preserve the angle they made with the pipe in the initial undeformed configuration.

Modelling of joints

A joint is introduced in the pipe model by specifying two elements instead of one at nodes where joints are present. The forces and moments arising from the relative displacements and rotations of the two elements are computed according to the constitutive behaviour (multi-linear) as obtained by experiment, with the unloading path assumed elastic with modulus equal to the tangent of the steepest slope of the constitutive behaviour curve.

One or more stages of the constitutive behaviour curve may have large gradients. These stages correspond to situations where the two pipe segments meeting at the joint come in direct contact, or in contact via a stiff joint part, i.e. become interlocked. In fact, since an experiment on a joint alone is practically impossible, such stages may be thought to correspond to deformations in the adjoining pipe segments used in the experiment. Given the time-stepping nature of the solution algorithm, that would require a decrease of the time step needed for stable computation. This is inefficient, so a special handling technique was developed for these stages. The displacement or rotation of one of the joint nodes is constrained to this of the other node until the next stage of the constitutive behaviour is entered. This is equivalent to approximating the original slope angle to 90° . Such stages are termed *locked*.

For obtaining the relative expansion or contraction an assumption needs to be made for the axial direction of joint displacement. This has been assumed to be the axis of one of the adjoining pipe segments, which is called the *reference beam*. It has been further assumed that a relative displacement between the joint nodes in the lateral direction does not occur.

Solution procedure

The solution is based on the double integration of the Newton equations of motion for each element. The motion of an element is considered uncoupled from the motion of the rest during a single time step, thus eliminating the need to assemble a stiffness matrix. An element then moves due to the out-of-balance force appearing on summation of the forces in all springs originating from it. For the system to reach equilibrium two types of damping are applied. First, the relative motion between elements is damped by a coefficient of damping calculated from the critical damping ratio of the material of the structure (steel, plastic, etc.). This is termed local damping. In addition, a small amount of viscous damping works on the absolute velocities of the elements. This is called global damping and represents the resistance of the medium in which the structure stands (soil). The method is inherently dynamic, geometrically non-linear, and can easily accommodate arbitrary amounts of rigid body motion thus providing numerically stable computation regardless of the number of broken springs in the course of analysis.

Verification

Experimental set-up and material properties

The applicability of the method to simulate the behaviour of an underground pipeline was verified by simulating an experiment, [9]. The outline of the experimental rig is given in Fig. 2. A PVC pipe with 100mm internal diameter, Young's modulus $E = 2.7\text{kN/mm}^2$ (linear elastic), and thickness $t=7.1\text{mm}$ is buried in a box filled with soil. Both ends of the pipe are firmly fixed to a steel frame attached to the box, restricting both translations and rotations. The left-hand side of the box subsides by 50cm at 1cm increments, resulting in deformation of the pipe. Strain gauges are mounted along the pipe at 60cm centres (indicated in the figure by circles). The joints are typical rubber ring (RR) joints with stoppers, with constitutive behaviour as shown in Fig. 3, (a) and (b). The bending constitutive behaviour of the pipe body as derived from three point bending test is shown in Fig. 3, (c).

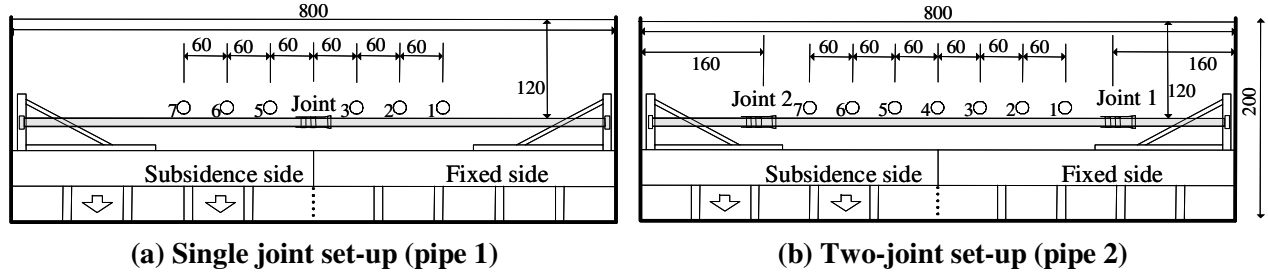


Fig. 2 Layout of experiment, [9]; units [cm]

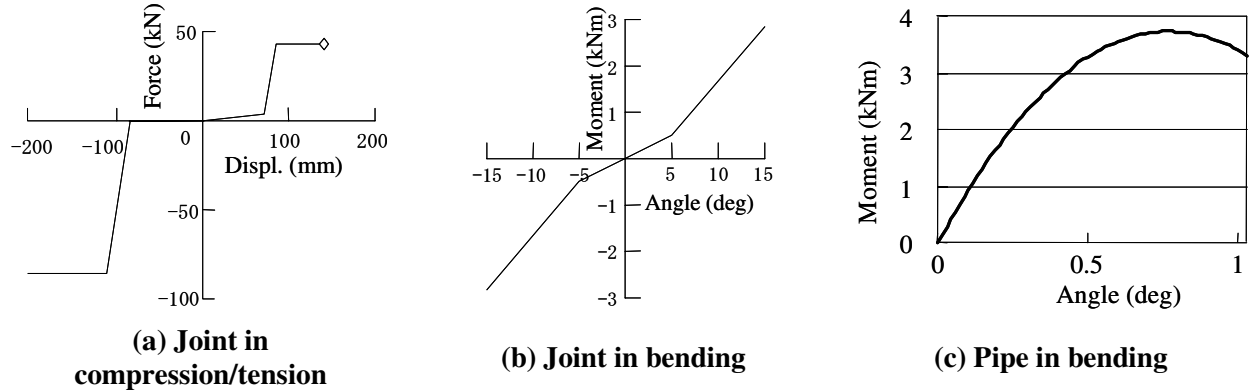


Fig. 3 Constitutive behaviour curves – PVC pipe, ϕ 100mm

Modelling details

The pipe length of 8m was divided into 80 segments, and 40 soil springs are used to represent the pipe-soil interaction in each of the three relevant directions, i.e. direct contact above and below the pipe and drag parallel to the pipe axis.

Two commonly used in Japan formulations for the soil springs are those of Takada et al, [10] and the Japan Gas Association (JGA) [11]; the parameters of direct contact springs for the two formulations and the soil used in the experiment are shown in Table 1. In the analyses, three formulations for the soil spring are used, the above two and a combination of them expected to yield better fit between experimental and analysis results than the original two formulations alone. In the results section below, the combined formulation is called *case 1*, the Takada formulation - *case 2* and the JGA formulation – *case 3*. For the combined formulation the best fit to experimental results is obtained when the JGA values are used for the fixed side, one-third of these values are used for the subsidence side, and additionally the slip limit $\Delta=4$ cm from Takada's formulation is imposed. This formulation was reached by trial and error analysis, while observing known facts such as the stiffness of springs at the fixed side being greater than at the subsidence side. The spring constant for the drag spring depends on the pipe material and the presence of joints; for PVC pipe with joints it is $k=3\text{N/cm}^3$, with onset of slip at 0.5cm [11].

Table 1. Formulations of direct contact springs

	Reference	Spring constant, k (per unit contact area)	onset of slip Δ
Subsidence side	Takada [10]	$k=1.96\text{N/cm}^3$	$\Delta=4.0\text{cm}$
	JGA [11]	Same as for the fixed side	
Fixed side	Takada [10]	Three times k for the subsidence side	not specified
	JGA [11]	$k=13.2\text{N/cm}^3$	$\Delta=0.5\text{cm}$

Results

In Fig. 4, the bending moment distributions obtained from the analyses are plotted together with the bending moments obtained from the experiment. From the charts it is understood that *case 1* and *case 3* results give good approximation to the experimental values.

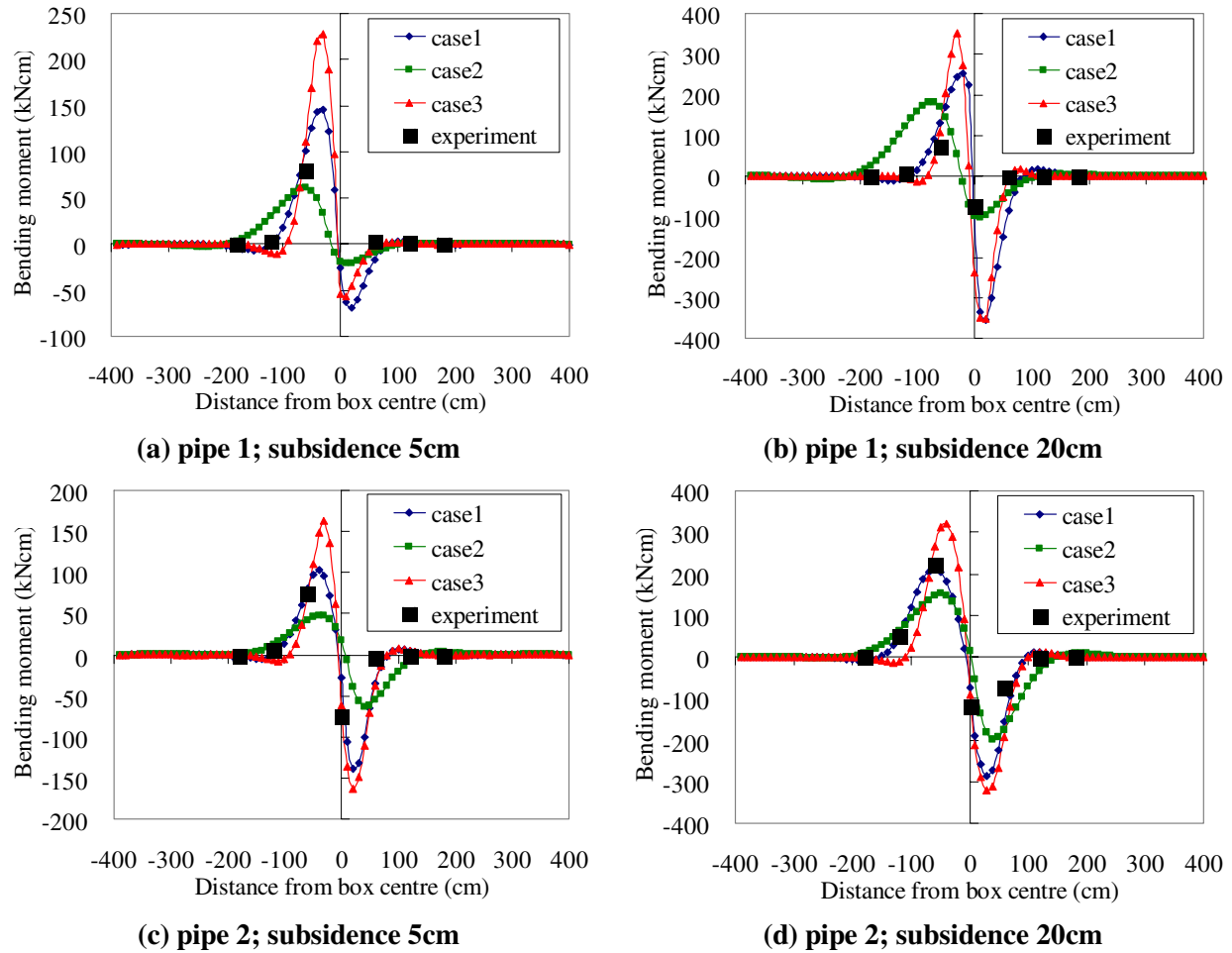
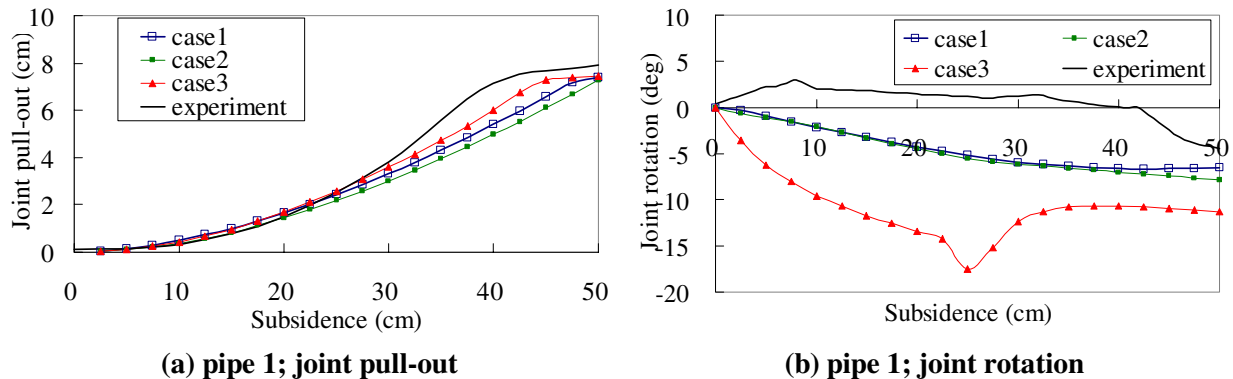


Fig. 4 Comparison of bending moments

In order to decide which of the two is better, a further comparison is made between the behaviour of joints yielded by analysis and the corresponding experimental values. The results are shown in Fig. 5. Rotations for pipe 2 are not shown since they are very small in absolute values. Clearly, the results for *case 1* are closer to the experimental values. All analyses hereafter are performed using formulation *case 1*.



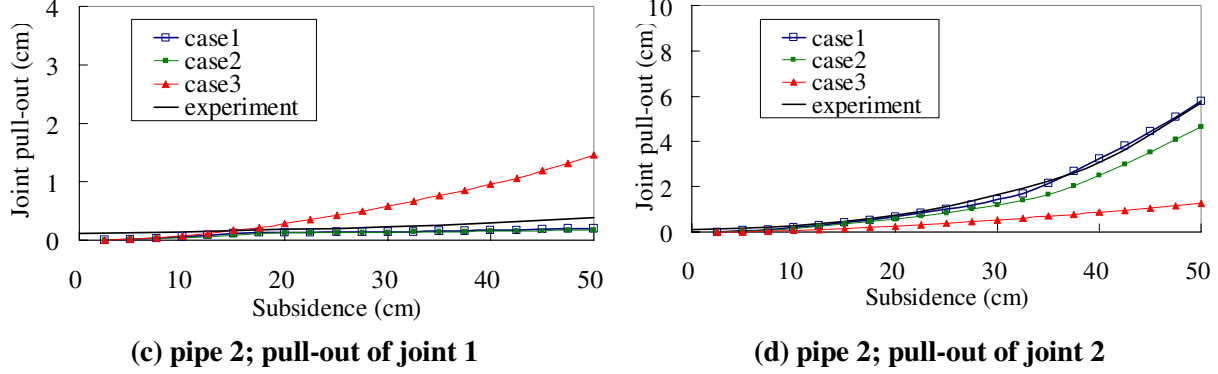


Fig. 5 Comparison of joint behaviour

CASE STUDIES

In this section we present the result of analyses for buried PVC jointed pipelines of three diameters, namely 75mm, 100mm and 150mm, subject to fault displacement, and discuss the influence of input parameters on the mode of failure and magnitude of fault slip causing failure.

Analysis model and input parameters

The model used for the analyses is shown in Fig. 6. The total length is 21m, this consisting of three 5m pipe segments connected by joints, and two 3m pipe segments. An equivalent spring is attached to the ends of the 3m segments to represent the pipe-soil interaction in the axial direction occurring beyond the model length. Fault displacement is applied between joints 1 and 2 at three different locations; at the middle of the central segment and 2m to the left and to the right of the midpoint. Further, the fault crossing angle α was varied for each crossing location from 30° to 150° at a step of 15° . The fault motion was applied downwards to the left-hand side of the model, so cases with crossing angles up to 90° correspond to normal faults, and above 90° to reverse faults.

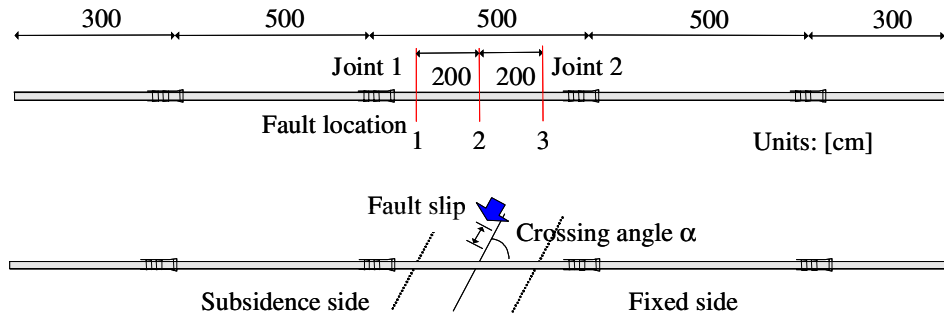


Fig. 6 Analysis model for case studies

Three types of soil were considered in order to cover the practical range of backfill material used in pipeline construction. The resulting parameters of soil springs are given in Table 2, the three soil conditions being K-1, K-2 and K-3. The actual stiffness of the direct springs k_v is computed from the following equation [11],

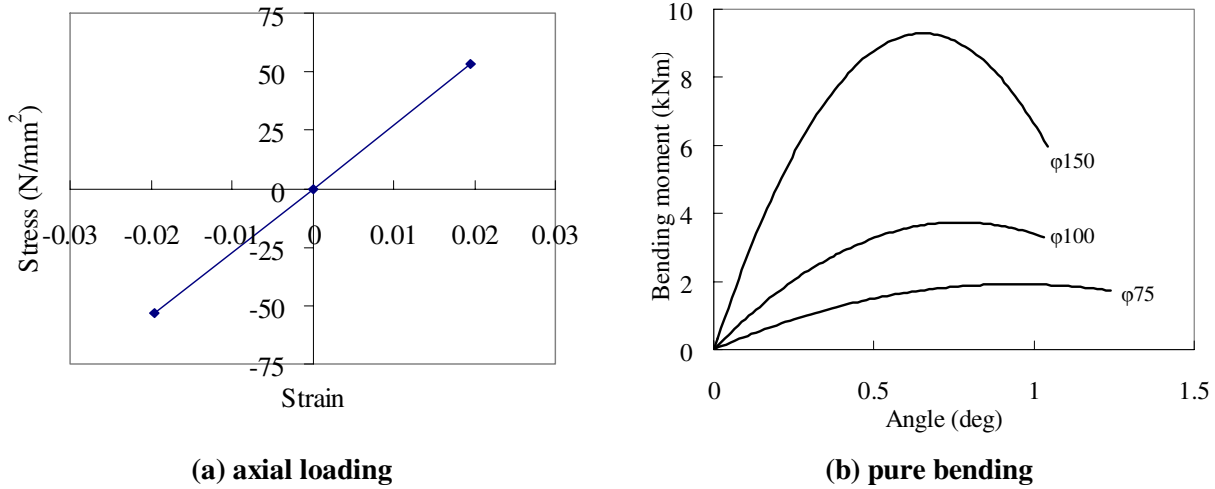
$$k_v = \frac{1}{3} \cdot K_{30} \cdot \left(\frac{D}{D_{150}} \right)^{-0.75} \quad (1)$$

where D is the external diameter of the pipe and D_{150} , the external diameter of a 150mm pipe.

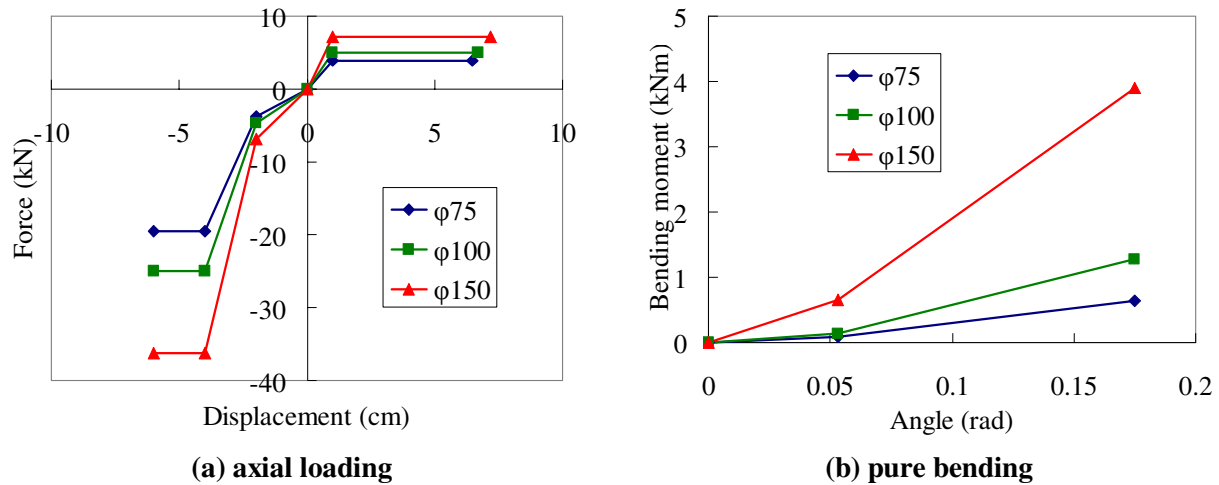
Table 2 Soil springs

Case	stiffness (N/cm ³)			onset of slip(cm)
	K-1	K-2	K-3	
Direct spring, K_{30} [11]	49	29.4	9.8	4.0
Drag spring	4.5	3	1.5	0.5

The stress-strain relationship of the PVC pipe material obtained from axial tension and compression test is shown in Fig. 7 (a). The behaviour is linear elastic with brittle failure. The moment-curvature relationship for the three pipes as derived from three-point bending tests is shown in Fig. 7 (b). The behaviour is strain softening without a notable yielding point. These curves were used in the analysis without simplifying assumptions.

**Fig. 7 Constitutive behaviour curves for the pipe body**

The constitutive behaviour of the joints in tension/compression is shown in Fig. 8 (a). The joints considered in the case studies are RR type but without stoppers, since the vast majority of pipes currently installed in Japan are equipped with such joints. A common feature of the joints is that they are strong in compression but weak in tension. The bending behaviour of the joints is shown in Fig. 8 (b).

**Fig. 7 Constitutive behaviour curves for joints**

Results

Failure modes

The failure modes for all analysis cases are summarised in Table 3. Seven distinctive failure types were observed, and designated in the table as follows: “1” for pull-out of joint 1; “-1” for pull-out of joint 2; “2” for compression failure of joint 1; “-2” for compression failure of joint 2; “0” for bending failure in the pipe body; “3” for bending failure of joint 1; “-3” for bending failure of joint 2.

Table 3 Failure modes

Fault location/ pipe type	Soil condition	Crossing angle (deg)								
		30	45	60	75	90	105	120	135	150
1/φ75	K-1	1	1	1	1	0	0	3	2	2
	K-2	1	1	1	1	3	3	3	2	2
	K-3	1	1	1	1	3	3	2	2	2
1/φ100	K-1	1	1	1	1	3	3	2	2	2
	K-2	1	1	1	1	3	3	2	2	2
	K-3	1	1	1	1	1	3	2	2	2
1/φ150	K-1	1	1	1	1	0	3	2	2	2
	K-2	1	1	1	1	0	3	2	2	2
	K-3	1	1	1	1	0	3	2	2	2
2/φ75	K-1	1	1	1	1	0	0	0	2	2
	K-2	1	1	1	1	0	0	2	2	2
	K-3	1	1	1	1	1	0	2	2	2
2/φ100	K-1	1	1	1	1	0	0	2	2	2
	K-2	1	1	1	1	0	0	2	2	2
	K-3	1	1	1	1	1	0	2	2	2
2/φ150	K-1	1	1	1	1	0	0	2	2	2
	K-2	1	1	1	1	0	0	2	2	2
	K-3	1	1	1	1	1	0	2	2	2
3/φ75	K-1	-1	-1	-1	-1	0	0	0	-2	-2
	K-2	-1	-1	-1	-1	0	0	0	-2	-2
	K-3	-1	-1	-1	-1	0	-3	-2	-2	-2
3/φ100	K-1	-1	-1	-1	-1	0	0	0	-2	-2
	K-2	-1	-1	-1	-1	0	0	-2	-2	-2
	K-3	-1	-1	-1	-1	-3	-3	-2	-2	-2
3/φ150	K-1	-1	-1	-1	-1	-1	-3	-2	-2	-2
	K-2	-1	-1	-1	-1	-1	-3	-2	-2	-2
	K-3	-1	-1	-1	-1	-1	-3	-2	-2	-2

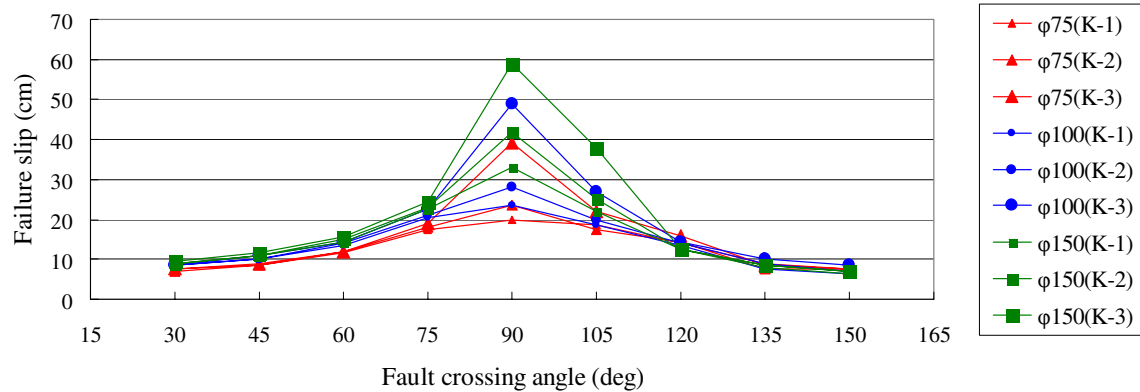
When the crossing angle is less than 75° the failure mode is always pull-out of a joint, regardless of the pipe diameter and the soil stiffness. Which joint pulls-out depends on the fault location, this being joint 1 for fault locations 1 and 2, and joint 2 for fault location 3. Likewise, for crossing angles greater than 135°, the failure mode is compressive failure of a joint. Which joint fails depends on the fault location in the same way it does for the pull-out failure.

The failure modes for crossing angles between 75° and 120° are more complex and depend on the pipe diameter, the soil stiffness and the crossing location. It can be seen from the above table that smaller diameter pipes are more likely to sustain bending failure at a joint for fault location 1, and less likely so for fault location 3. The reason for this is the greater stiffness of the soil at the fixed side of the model which makes the rotation of joint 2 more difficult. On the other hand, the rotation at joint 1 is facilitated by the

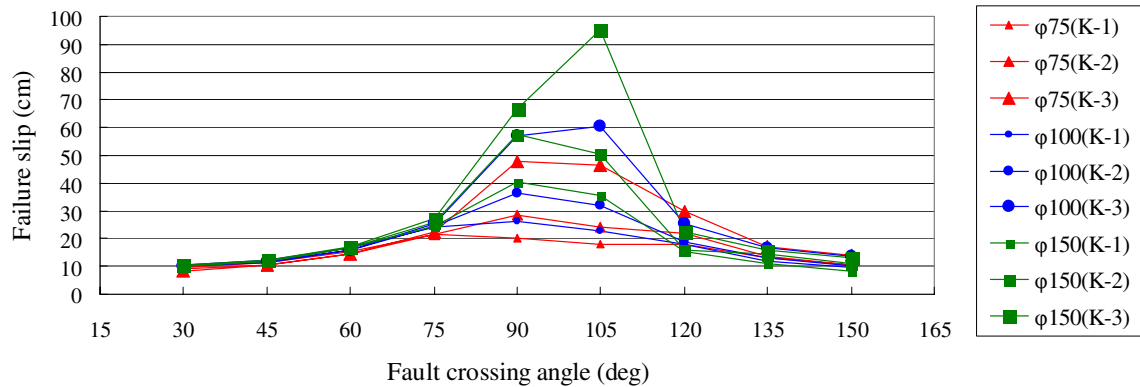
proximity of the fault location 1 together with the small stiffness of soil at the subsidence side. Thus in this crossing angle range the failure is localised for the small diameter pipes causing failure by bending in the pipe body. For the 150mm pipe the pipe stiffness is great enough to avoid localization, so the mode of failure is different. For crossing angle 90° in particular, the failure mode depends on the soil stiffness and is bending failure in the pipe body for stiff soil, and joint pull-out for soft soil.

Relation between fault location/crossing angle and slip at failure.

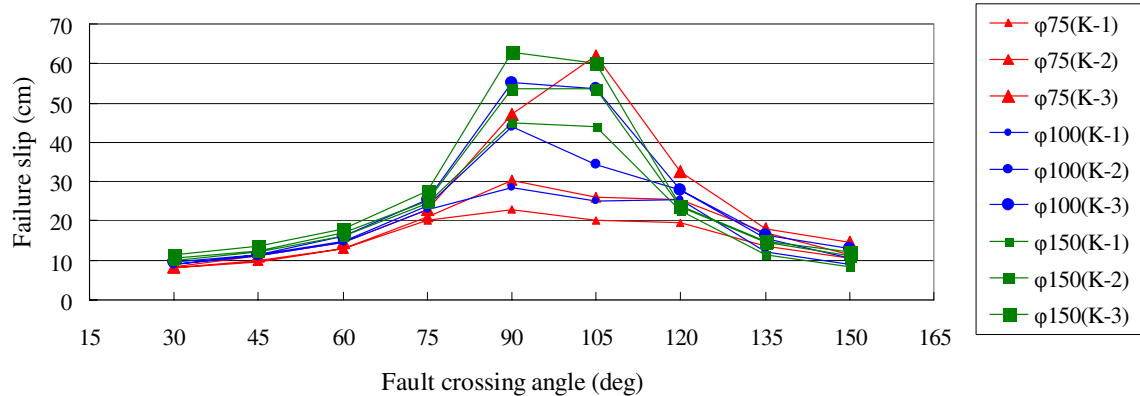
The fault slip at failure obtained from the analyses for each pipe, soil condition and crossing angle is shown in Fig. 8; one chart for each fault crossing location .



(a) Fault location 1



(b) Fault location 2



(c) Fault location 3




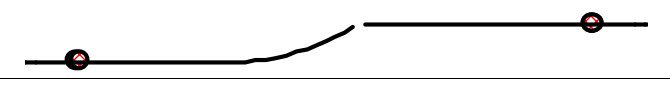
Fig. 8 Slip at failure

The general trend observed is that all pipes have highest resistance against fault motion for crossing angles close to 90° , and lowest resistance when the crossing angle is near to 30° or 150° . Further there is not much difference in the resistance in the ranges $30^\circ\sim 75^\circ$ and $120^\circ\sim 150^\circ$, regardless of the pipe diameter, the stiffness of soil and the fault crossing location. Bearing in mind that for these ranges the mode of failure is either pull-out or compression failure of the joints, the fault slip at failure is obviously governed by the amount of expansion/contraction allowance of the joints and the component of fault motion parallel to the pipe axis. When the crossing angle is close to 90° , the highest resistance occurs for soft soil and stiff pipes, i.e. when the strain localization is avoided.

The 105° case is the only one for which pull-out and compression failure does not occur. For this angle, the shrinking deflection of joint 1 caused by the parallel component of fault displacement is cancelled-out by the expansion caused by the transverse component of fault displacement. On the other hand the elongation allowance of joint 2 is still not reached when failure occurs (bending of the pipe or joint). Therefore, the effect of soil conditions and pipe bending stiffness is the greatest for this crossing angle. Among the three fault crossing locations for 105° the largest resistance occurs for location 2, i.e. when the joints are away from the fault. In this case the deformation of the joints is minimal, resulting in failure only by bending in the pipe body.

Deformed shapes for the various modes of failure are shown in Table 4. The conditions in the last column are in the following order: pipe diameter/crossing location/ crossing angle/soil condition.

Table 4 Characteristic deformed shapes

Failure mode	Deformed shape	Conditions
Joint pull-out		$\phi 75/2/90^\circ/K-3$
Joint compression		$\phi 150/3/120^\circ/K-3$
Joint bending		$\phi 150/3/105^\circ/K-3$
Pipe bending		$\phi 75/2/90^\circ/K-2$

SIMPLIFIED METHOD FOR ESTIMATION OF THE RESISTANCE TO FAULT SLIP

In this section we derive equations for determining the fault slip at failure without needing to perform analysis by considering the parameters influencing the pipe behaviour (pipe type, soil stiffness, joint properties, fault crossing location and angle).

It was observed in the case studies that for crossing angles 90° , if a joint is sufficiently away from the fault location, bending failure at a joint does not occur. First, we seek to find what conditions need to be satisfied in terms of fault location for bending failure at a joint to be avoided. A typical bending moment diagram for crossing angle 90° is shown in Fig. 9. At the limit state when the bending moment in the pipe reaches its bending capacity, failure at a joint would not occur if the joint is at a distance l_a to the left of

the fault location or at a distance l_b to the right of the fault location. A best-fit optimization analysis was performed to find expressions for the values of l_a and l_b , which resulted in the following equations,

$$l_a = \frac{198}{k_v} + 4M_h + 0.02I + 59 \quad (2)$$

$$l_b = \frac{124}{k_v} + 52M_h - 0.2I + 40 \quad (3)$$

where M_h is the bending capacity of the joint, and I is the second moment of area of the pipe section. The data sets used to obtain these equations were all analyses for which bending failure of the joints did occur. Since only three fault crossing locations were considered in the case studies, further analyses were carried out for pipe $\phi 100$, soil condition K-2, crossing angle 90° , and fault crossing 40cm, 60cm, 80cm and 100cm to the left of joint 1. For this setting, the value calculated from equation 2 is 75.1cm. On the other hand, when the fault was 60cm away from the joint it did fail in bending, and at 80cm the joint did not fail. The correlation between predicted and analysis values is shown in Fig. 10, and is thought to be good enough for practical use.

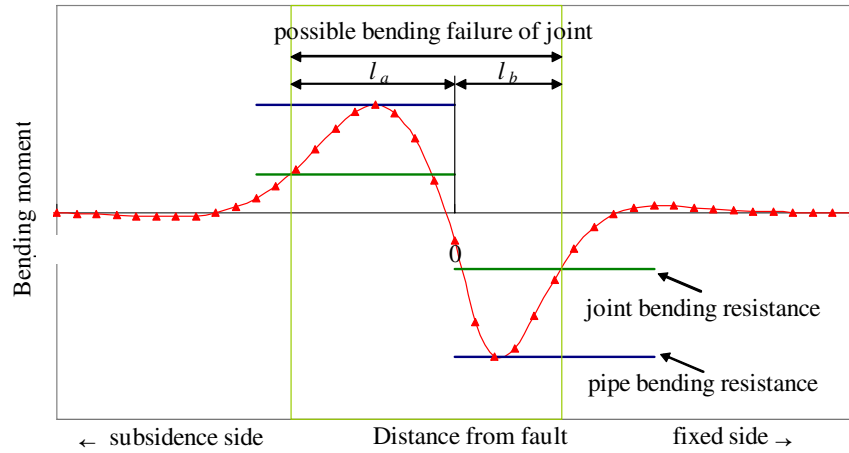
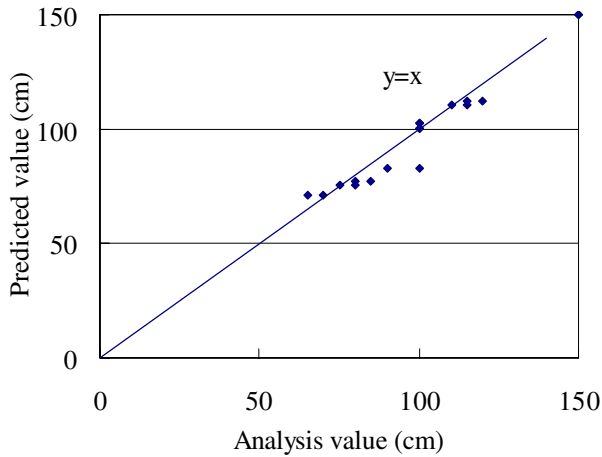
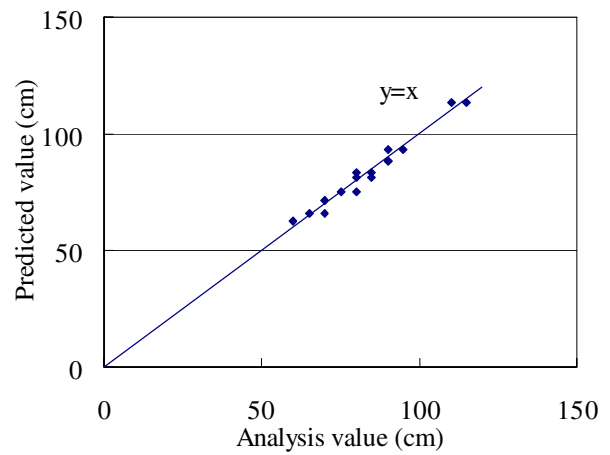


Fig. 9 Region in the fault vicinity where a joint may fail in bending



(a) subsidence side; l_a



(b) fixed side; l_b

Fig. 10 Correlation between predicted and analysis values of l_a and l_b

Having defined l_a and l_b , we proceed to derive equations for the failure slip. In doing this we again take advantage of the observations made on the case studies results. It is convenient to first decide on possible failure modes according to the crossing angle, further narrow the scope of possible modes according to the crossing location, and only then perform best-fit analysis among the relevant data sets obtained from the case studies. According to the failure mode the fault slip at failure has been designated as shown in Table 5. The procedure for computing the failure slip Y is shown in Fig. 11. The symbols l_1 and l_2 in the figure stand for the distance from the fault to the joint in the subsidence side and the fixed side respectively.

Table 5 Failure slip naming convention

Symbol	Failure mode
X_0	Bending of pipe body
X_1	Pull-out of joint ($\alpha < 75^\circ$)
X_1'	Pull-out of joint ($75^\circ < \alpha < 90^\circ$)
X_2	Compression of joint
X_3	Bending of joint ($75^\circ < \alpha < 90^\circ$)
X_3'	Bending of joint ($90^\circ < \alpha < 135^\circ$)

When the crossing angle is less than 75° (normal fault) the failure mode is uniquely defined as joint pull-out. When the crossing angle is greater than 135° (reverse fault), the failure mode is joint compression. When the crossing angle is between 75° and 135° (close to 90°), there are several possibilities according to the fault crossing location. If the crossing location is close enough to a joint the minimum value from three possible modes of failure is chosen. If not, then only two modes of failure are possible, i.e. bending of the pipe body, and joint pull-out or compression.

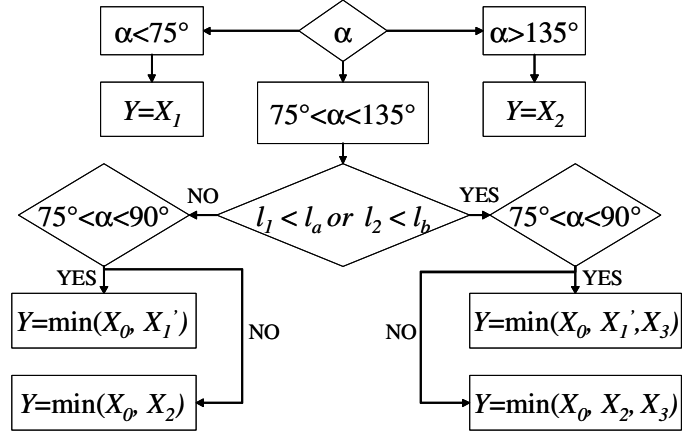


Fig. 11 Flow-chart for computing the slip at failure

The equations obtained from best-fit analysis are as follows:

$$X_1 = \frac{5}{\cos \alpha} + 3.3\delta_{max} + \frac{4.8}{k_v} - 18.6 \quad (4)$$

$$X_1' = 853.2 \sin \alpha + 21.5\delta_{max} + \frac{21.6}{k_v} - 0.015I - 945 \quad (5)$$

$$X_2 = \frac{-12.5}{\cos \alpha} - 3.3\sigma_c + \frac{15.8}{k_v} + 0.089l_1 - 17.8 \quad (6)$$

$$X_3 = 36.8 \sin \alpha + \frac{58.8}{k_v} + 0.35l_1 + 0.7M_h - 24.5 \quad (7)$$

$$X_3' = 1.78 \sin \alpha + \frac{65.7}{k_v} + 0.24l_1 + 1.6M_h + 20.3 \quad (8)$$

$$X_0 = 18.7 \sin \alpha + \frac{171}{k_v} + 0.018I - 3.2 \quad (9)$$

where δ_{max} is the pull-out allowance of the joint, and σ_c is the compression stress at failure of the joint. In the equations, the unit of force should be kN , unit of angle – rad and the unit of length cm . The only exception is k_v , which should be in N/cm^3 .

The correlation of failure displacements computed by the above equations and the corresponding failure values yielded by the case studies is shown in Fig. 12. The correlation is sufficient for practical use, and the computed values tend to be on the conservative side. An example of the fragility curves computed by the equations is shown in Fig. 13. The failure slip for a particular crossing angle is the minimum of all values obtained from curves relevant to the crossing angle, e.g. 25.5cm for crossing angle 120°.

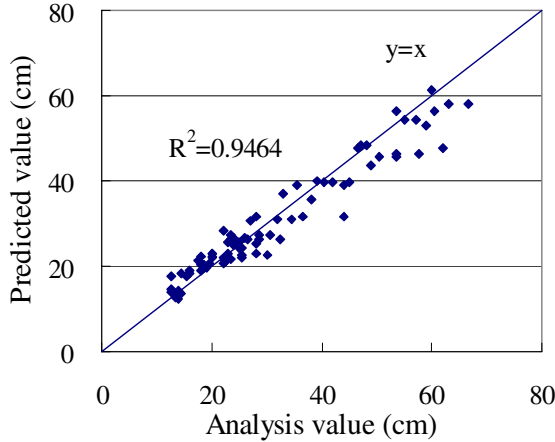


Fig. 12 Correlation between predicted and analysis values of fault slip at failure

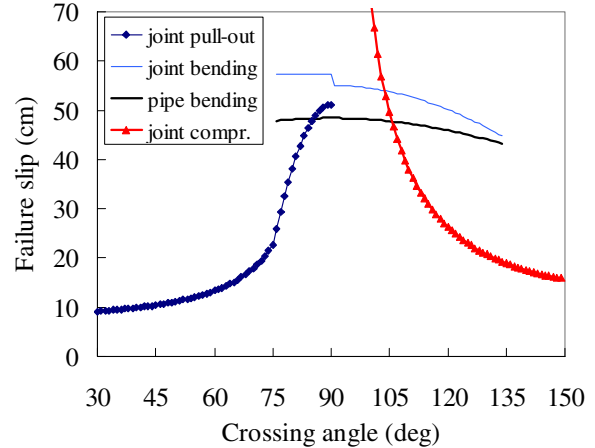


Fig. 13 Fragility curves; pipe ϕ 75mm, soil K-3, crossing location 3

CONCLUSIONS

An efficient numerical method for modelling of jointed underground pipes was introduced. The merits of the method are the possibility to use any type of constitutive behaviour for the pipe material, joints and the soil, making it completely nonlinear in terms of material behaviour. The method is also geometrically nonlinear and allows stable computation for any magnitude of displacements and any amount of damage to the model in terms of pipe body failure, joint failure or soil failure. At the same time the use of line elements allows fast computation and easy interpretation of results. The developed program can be used by pipe and fittings manufacturers for testing the performance of new jointing techniques.

Proper modelling of pipe-soil interaction is essential for producing meaningful results when the soil is simplified to equivalent springs. To this end, verification against experimental data was done, and an optimum formulation for the springs representing the surrounding soil producing good fit between analysis and experimental results was identified. The formulation is based on combining recommendations from past research on this matter, so it can be considered reliable for use in analyses other than the experimental verification itself.

Case studies were carried-out for three most commonly used PVC pipe diameters, and a range of soil conditions, fault crossing angles and fault crossing locations. The possible failure modes were identified as well as the combinations of analysis parameters leading to a particular failure mode. For crossing angles in the ranges 30° to 75° and 120° to 150° the failure modes are exclusively joint pull-out and joint compression respectively. For these ranges the influence of soil stiffness, and fault crossing location is negligibly small. The failure appears to depend simply on the amount of pull-out or compression allowance of the particular joint. Therefore, for these crossing angle ranges little can be done in terms of failure countermeasures, but to increase the joint axial movement allowances.

For the crossing angle range 75° to 120° the failure mode can vary from joint pull-out (up to 90°), through bending failure of the pipe body or joint (90° to 120°) to joint compression failure (120°). The actual failure mode in this range is strongly dependent on the soil stiffness and the fault crossing location. Stiffer soil leads to bending moment localization and bending failure in the pipe is more likely than joint failure, i.e. for large soil stiffness to pipe stiffness ratio the behaviour of a jointed pipe is similar to the behaviour of the same pipe without joints even when the fault crossing location is as close as 50cm to a joint. On the other hand, for softer soils bending moment localization does not occur and joints may fail before the pipe does. Depending on the conditions, the failure slip in this range can be between two and ten times as large as the failure slip at crossing angles 30° or 150° . Therefore, significant improvement in the performance can be achieved if pipes are placed so as to cross a known fault at angles close to 90° , without resorting to measures such as using softer backfill, improving the resistance of the pipe, or using special joints or more joints in the fault vicinity.

Simple parametric equations were derived for predicting the failure slip. By using one equation per specific fault crossing angle range and fault crossing location, good fit was obtained between analysis and predicted displacements. The proposed equations are useful for damage estimation studies for actual and scenario earthquakes.

ACKNOWLEDGEMENTS

The cooperation of Dr. Shin Katagiri from Kubota Corporation, Japan in providing experimental data for PVC pipes and joints is highly appreciated. This research would not have been possible without it.

REFERENCES

1. Kobe University engineering survey team. "Kobe earthquake emergency survey report – Part 2." Kobe University: Civil Engineering Department, 1995 : 13-9 (*in Japanese*)
2. Kobe earthquake damage survey committee. "Kobe earthquake damage survey report - damage to civil structures.", JSCE, 1998 (*in Japanese*)
3. Niigata earthquake damage survey committee. "Niigata earthquake damage survey report - damage to civil structures.", JSCE, 1966 (*in Japanese*)
4. Ministry of construction; Civil engineering research institute. "Niigata earthquake damage survey report" No. 125, 1965 (*in Japanese*)
5. Kennedy R, Chow AW, and William RA. "Fault movement effects on buried oil pipeline.", ASCE: Transportation Engineering Journal, 1977; Vol. 103, No. TES, 617-33
6. Wang LR, and Wang LJ. "Parametric study of buried pipelines due to large fault movement." ASCE: TCLEE, 1995; No.6, 152-59
7. Takada S, Hassani N and Fukuda K. "A new proposal for simplified design on buried steel pipes crossing active faults.", JSCE: Journal of Structural Mechanics and Earthquake Engineering, 2001; Vol. 668, No. 54, 187-94
8. Takada S, and Tanabe K. "Three dimensional seismic response analysis of buried continuous or jointed pipelines.", ASME: Journal of Pressure Vessel Technology, 1987; Vol. 109, No. 54, 80-7,.
9. Takada S, Nakano M, Katagiri S, Tani K, Koyanagi S. "Experimental behaviour of a PVC pipe subjected to non-uniform subsidence during earthquake." Proceedings of the Japanese Society of Civil Engineers, 1999; Vol. 619, 145-54 (*in Japanese*)
10. Takada S, Tanabe K, Hazama Y, Irioka H. "Experimental behaviour of a pipe attached to a manhole, and development of seismic countermeasures.", Proceedings of the Japanese Society of Civil Engineers, 1986; Vol. 374, pp.575-82 (*in Japanese*)
11. Japan Gas Association. "Manual for aseismic design of gas distribution pipelines.", 1982